ApJ vol. 551 - Apr 20, 2001 issue, in press

VLBI Observations of a Complete Sample of Radio Galaxies. 10 Years Later

G. Giovannini[1,2], W.D. Cotton[3], L. Feretti[2], L. Lara[4], and T. Venturi[2]

ABSTRACT

A complete sample of 27 radio galaxies was selected from the B2 and 3CR catalogs, in order to study their properties on the milliarcsecond scale. In the Appendix of this paper we present new radio images for 12 of them. Thanks to the present data, all the sources in this sample have been imaged at mas resolution. We discuss the general results. In particular we stress the evidence for high velocity jets in low power radio galaxies, we compare high and low power sources, and discuss the source properties in the light of the unified scheme models. We derive that the properties of parsec scale jets are similar in sources with different total radio power and kpc scale morphology.

From the core - total radio power correlation, we estimate that relativistic jets with Lorentz factor γ in the range 3 - 10 are present in high and low power radio sources. We discuss also the possible existence of a two velocity structure in parsec scale jets (fast spine and lower velocity external shear layer).

Subject headings: galaxies: active — galaxies: jets — galaxies: nuclei — radio continuum: galaxies

1. Introduction

The study of the parsec scale properties of radio galaxies is crucial to obtain information on the nature of their central engine, and provides the basis of the current *unified theories* (see e.g. (Urry & Padovani 1995)), which suggest that the appearance of active galactic nuclei strongly depends on orientation. In the *high-luminosity unified scheme*, quasars and powerful radio galaxies (FR II, (Fanaroff & Riley 1974)) are suggested to be the same class of objects but seen at different viewing

[1]Dipartimento di Fisica, Universita' di Bologna,via B.Pichat 6/2, 40127 Bologna, Italy

[2]Istituto di Radioastronomia del CNR, via Gobetti 101, 40129 Bologna, Italy

[3]National Radio Astronomy Observatory, 520 Edgemont Rd, Charlottesville VA 22903-2475, USA

[4]Instituto de Astrofísica de Andalucía, CSIC, Apdo 3004, 18080 Granada, Spain

angles. Similarly, the *low-luminosity unified scheme* assumes BL-Lacs to be the beamed population of radio galaxies of low-intermediate luminosity (FR I).

To get new insight in the study of radio galaxies at pc resolution, we undertook a project of observations of a complete sample of radio galaxies selected from the B2 and 3CR catalogs (Giovannini et al. 1990). Since both catalogs have been selected at low frequencies, the source properties are dominated by the unbeamed extended emission and are not affected by observational biases related to orientation effects.

In the Appendix we present new images and data for 12 galaxies of our sample and give short notes reviewing also published results. After 10 years high quality images and data are available for all sources in the sample, so that we can derive and discuss general properties of the whole sample.

We will use here a Hubble constant $H_0 = 50$ km sec^{-1} Mpc^{-1} and a deceleration parameter $q_0 = 0.5$ (note that different cosmological constants have been used in previous papers on the same sample).

2. The Sample

In Table 1 we give the list of radio galaxies. The complete sample (Giovannini et al. 1990), consisting of 27 radio galaxies from the B2 and 3CR catalogs, satisfies the following criteria:

Declination $> 10°$

Galactic latitude b > 15 °

Arc-second core flux density at 5 GHz (S_c) ≥ 100 mJy

Apparent visual magnitude of the associated galaxy $m_v \leq 20$, for 3CR sources.

With respect to the original list presented in Giovannini et al. (1990), we give a more accurate flux density measurement of the core at arc-second resolution, when available, to minimize the contamination from the jet(s) flux density. The total radio power has been scaled according to the different cosmological parameters used here.

The selection criterion of restricting the sample to the radio galaxies with a relatively high core flux density limit ($\gtrsim$100 mJy at 6 cm), was adopted for obvious observational reasons at the time of the sample selection. We are aware that it results in a selection effect in favor of objects with a beamed core i.e. oriented at a small angle with respect to the line of sight. Despite this effect, the sample is dominated by low-intermediate power FR I radio galaxies and by extended steep spectrum FR II radio galaxies. The VLBI study of a sample selected without any restrictions on the core flux density is in progress.

In Fig. 1 we show a plot of the observed core power versus total radio power for the present sample. The line represents the correlation found by Giovannini et al. (1988). As expected from

Table 1. The Selected Sample

Name IAU	Name other	z	$S_c(5.0)$ mJy	Log P_t W/Hz	Type	References
0055+30	NGC315	0.0167	588	24.56	FR-I	1
0104+32	3C31	0.0169	92	25.11	FR-I	2
0116+31	4C31.04	0.0592	32	25.71	CSO	3 *
0206+35	4C35.03	0.0375	106	25.46	FR-I	2
0220+43	3C66B	0.0215	182	25.59	FR-I	*
0222+36		0.0327	122	24.20	LPC	*
0258+35	NGC1167	0.0160	$\lesssim$243	24.65	CSS	*
0331+39	4C39.12	0.0202	149	24.49	LPC	*
0410+11	3C109.0	0.3056	244	27.78	FR-II	4
0648+27		0.0409	213	24.31	LPC	*
0755+37	NGC2484	0.0413	195	25.65	FR-I	4
0836+29	4C29.30	0.0790	152	25.70	FR-I	5
1101+38	Mkn 421	0.0300	640	24.66	BL-Lac	6
1142+20	3C264	0.0206	200	25.46	FR-I	2
1144+35		0.0630	450	24.95	FR-I	7
1217+29	NGC4278	0.0021	63	21.44	LPC	*
1222+13	3C272.1	0.0037	180	23.27	FR-I	*
1228+12	3C274	0.0037	4000	25.07	FR-I	8
1322+36	NGC5141	0.0175	150	24.36	FR-I	*
1441+52	3C303	0.1410	181	26.74	FR-II	*
1626+39	3C338	0.0303	105	25.86	FR-I	9
1641+17	3C346	0.1620	220	26.98	FR-II	3
1652+39	Mkn 501	0.0337	1250	24.96	BL-Lac	6
1833+32	3C382	0.0586	188	26.31	FR-II	4 *
1845+79	3C390.3	0.0569	340	26.58	FR-II	10
2243+39	3C452.0	0.0811	130	26.92	FR-II	*
2335+26	3C465	0.0301	246	25.91	FR-I	5

Note. — $S_c(5.0)$ is the arc-second core flux density at 5.0 GHz; Log P_t is the logarithmic of the total radio power at 408 MHz. **References**: main reference to published VLBI data: 1 - Cotton et al. (1999); 2 - Lara et al. (1997); 3 - Cotton et al. (1995); 4 - Giovannini et al. (1994); 5 - Venturi et al. (1995); 6 - Giovannini et al. (1999b); 7 - Giovannini et al. (1999a); 8 - Junor et al. (1999), and Biretta et al. (1999); 9 - Giovannini et al. (1998a); 10 - Alef et al. (1996); an * is given when new data are presented in this paper

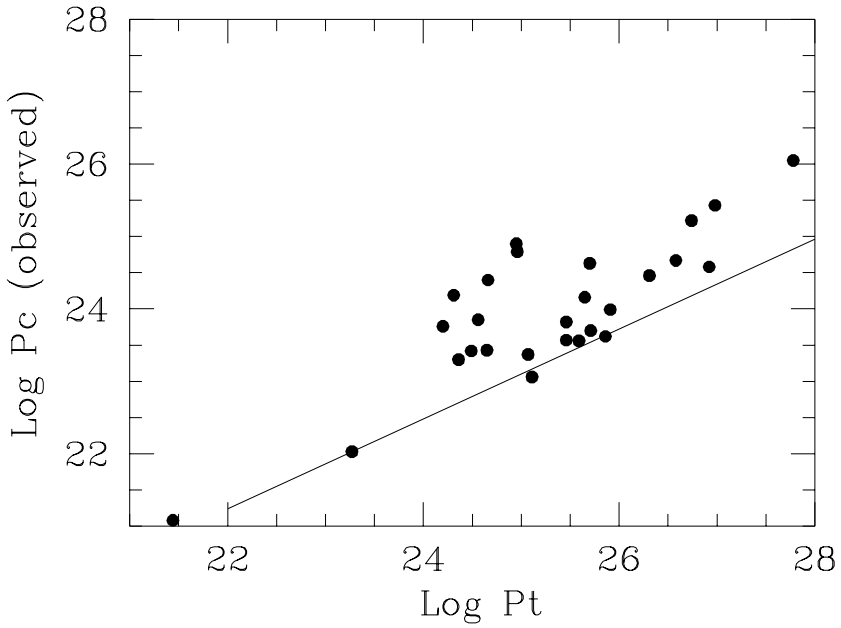

Fig. 1.— Total radio power at 408 MHz versus the observed arc-second core radio power at 5 GHz. The continuum line represents the correlation between the core and total radio power found by Giovannini et al. (1988).

the core flux density selection effect, most of present sources have a core radio power higher than average with respect to their total radio power.

3. Constraints on the jet orientation and velocity

We will use the available observational data to constrain the jet velocity and orientation for all the sources of our sample. In the following we briefly summarize the methods used. Other methods are possible e.g. the X-ray non thermal nuclear emission could be used to derive a possible Doppler factor according to the Synchrotron-Self-Compton model (see e.g. Giovannini et al. (1994)). However, they do not give significant limits because of the large uncertainties in the available data.

3.1. Jet Sidedness

Assuming that the jets are intrinsically symmetric, the jet velocity (βc) and orientation (θ), can be constrained from the jet to counter jet brightness ratio R, according to the formula

$$R = (1 + \beta \cos\theta)^{2+\alpha} \ (1 - \beta \cos\theta)^{-(2+\alpha)}$$

We assume a jet spectral index $\alpha = 0.5$ with $S \propto \nu^{-\alpha}$. The validity of this formula depends on the degree of isotropy of the intrinsic synchrotron emissivity in the jets. Here we assume that the parsec scale jet emissivity is isotropic (see Giovannini et al. (1994) for a more detailed discussion).

3.2. Core Dominance

Giovannini et al. (1988) found a general correlation between the core and total radio power in radio galaxies. Since the total radio power was measured at low frequency and is therefore not affected by Doppler boosting, the core emission derived by the total radio power is not boosted. Assuming that sources are oriented at random angles the best fit value corresponds to the average orientation angle (60°) and the observed dispersion of the core radio power around the best fit line reflects the different orientation angles (see Giovannini et al. (1994) for a more detailed discussion). We can use this correlation to derive the expected intrinsic core radio power from the total galaxy radio power and, comparing it with the observed core radio power, to estimate the source orientation.

Here we have re-analyzed the correlation given in Giovannini et al. (1988) to take into account new better quality data of the core flux density at 5 GHz. Moreover, we added the radio quasars with the same selection criteria used for radio galaxies, since all sources with θ in the range 0° - 90° should be included, to derive the correct correlation. The new correlation (scaled for the different cosmological constants used here) is very similar to the previous one:

$$\log P_c = (0.62 \pm 0.04) \log P_t + (7.6 \pm 1.1)$$

where P_c is the arc-second core radio power at 5 GHz and P_t is the total radio power at 408 MHz. To take into account the core variability, we have allowed the core flux density to vary within a factor of two from the measured one.

3.3. Proper Motion

Proper motion is detected in 7 sources, for which we can derive the apparent velocity β_a c. From this value we can constrain the intrinsic jet velocity and orientation as follows:

$$\beta = \beta_a/(\beta_a \cos\theta + \sin\theta)$$

.

In this paper we will assume that the jet bulk velocity and the pattern velocity have comparable values (see e.g. Ghisellini et al. (1993)).

4. Results

In Table 2 and Figures 2 and 3, we give for each source the estimated range of the jet velocity and orientation with respect to the line of sight derived from the methods previously discussed.

In most sources the allowed ranges in jet velocity and/or orientation are large because of: i) the low brightness of the jets, ii) the uncertainties in the core dominance related to the possible core flux density variability, iii) the lack of measured proper motion. For 2 sources of our sample (0258+35 and 1217+29), we cannot give any constraint, therefore we have a working sample of 25 sources.

4.1. FR I Radio Galaxies

In the present sample, there are 13 FR I radio galaxies: one (3C338) shows a clear two-sided structure, three show a short counter-jet (NGC 315, 3C66B, and 1144+35), and nine have a one-sided morphology.

In all the FR I sources, the jets are relativistic, β being always larger than 0.5 and in four cases > 0.9 (Fig. 2). Proper motion has been measured in four sources (Table 2), and could probably be found in other sources but it requires a larger observational effort. The jet orientation is in agreement with the expectations of the unified model: θ is $> 30^\circ$ for six sources while in five sources we do not have strong constraints on θ which could be $> 30^\circ$, but smaller values cannot be excluded. In 3C 274 and 1144+35 a viewing angle smaller than 30° is obtained (Fig. 3). However,

Table 2. Jet velocity and orientation - estimated parameters

Name IAU	Name other	Type	θ range degree	β range v/c	γ range	Motion β_a
0055+30	NGC 315	FR I	30 - 40	> 0.8	> 1.7	1.13 - 2.51
0104+32	3C 31	FR I	40 - 60	> 0.7	> 1.4	
0116+31	4C31.04	CSO	> 75	any	–	
0206+35	4C35.03	FR I	< 54	> 0.5	> 1.15	
0220+43	3C66B	FR I	~ 45	0.6 - 0.99	1.25 - 7.09	
0222+36		LPC	< 40	> 0.7	> 1.4	
0258+35	NGC 1167	CSS	–	–	–	
0331+39	4C39.12	LPC	< 45	> 0.5	> 1.15	
0410+11	3C 109	FR II	10 - 35	> 0.8	> 1.7	
0648+27		LPC	< 40	> 0.7	> 1.4	
0755+37	NGC 2484	FR I	< 45	> 0.6	> 1.25	
0836+29	4C29.30	FR I	< 35	> 0.55	> 1.20	
1101+38	Mkn 421	BL-Lac	< 30	> 0.87	> 2.03	1.5
1142+20	3C 264	FR I	~ 50	~ 0.98	~ 5.0	
1144+35		FR I	20 - 25	≥ 0.95	≥ 3.2	2.7
1217+29	NGC 4278	LPC	–	–	–	
1222+13	3C 272.1	FR I	60 - 65	$\gtrsim 0.9$	≥ 2.29	
1228+12	3C 274	FR I	< 19	$\gtrsim 0.99$	$\gtrsim 6$	6
1322+36	NGC 5141	FR I	$\lesssim 58$	$\gtrsim 0.54$	$\gtrsim 1.19$	
1441+52	3C 303	FR II	≤ 40	≥ 0.7	> 1.4	
1626+39	3C 338	FR I	~ 85	~ 0.8	~ 1.7	0.8 - 0.9
1641+17	3C 346	FR II	< 30	> 0.8	> 1.7	
1652+39	Mkn 501	BL-Lac	10 - 15	> 0.99 - 0.999	7.09 - 22.4	4 - 8
1833+32	3C 382	FR II	< 45	> 0.6	> 1.25	
1845+79	3C 390.3	FR II	30 - 35	> 0.96	> 2.29	3.5
2243+39	3C 452	FR II	$\gtrsim 60$	> 0.4	> 1.09	
2335+26	3C 465	FR I	$\lesssim 54$	> 0.6	> 1.25	

Note. — θ gives the allowed values for the jet orientation with respect to the line of sight. β and γ gives the allowed values for the jet velocity. β_a c is the measure of the apparent velocity, where available.

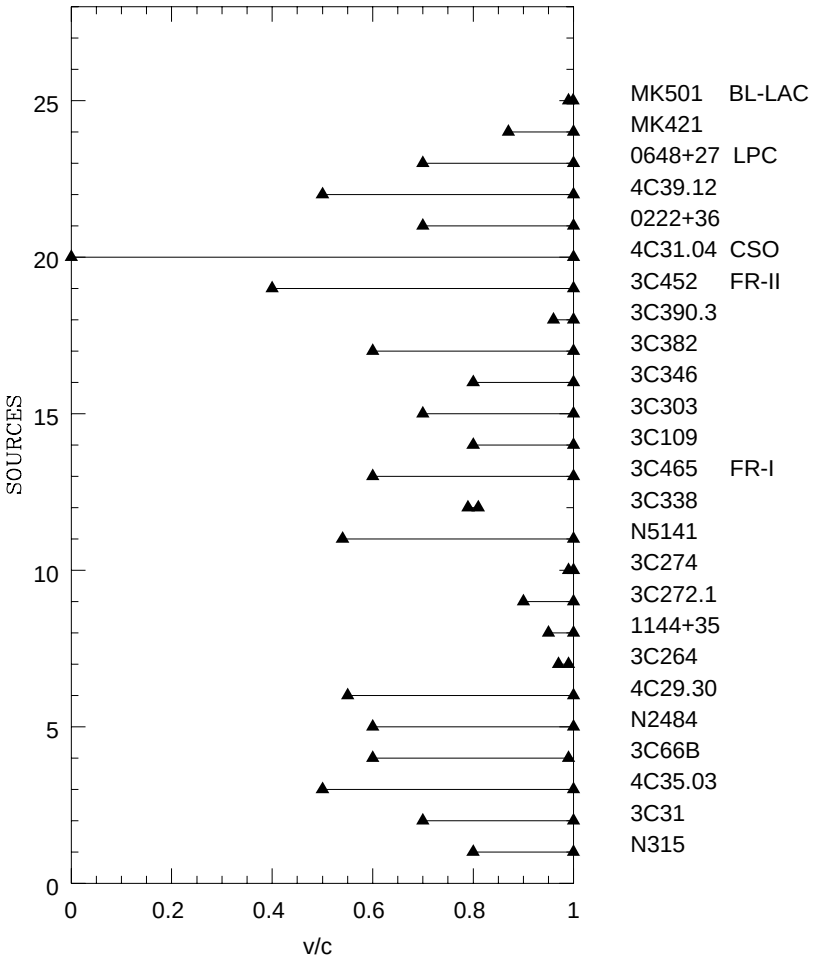

Fig. 2.— Allowed range of the jet velocity β = v/c for different sources. Note that sources are grouped together according to their large scale radio morphology.

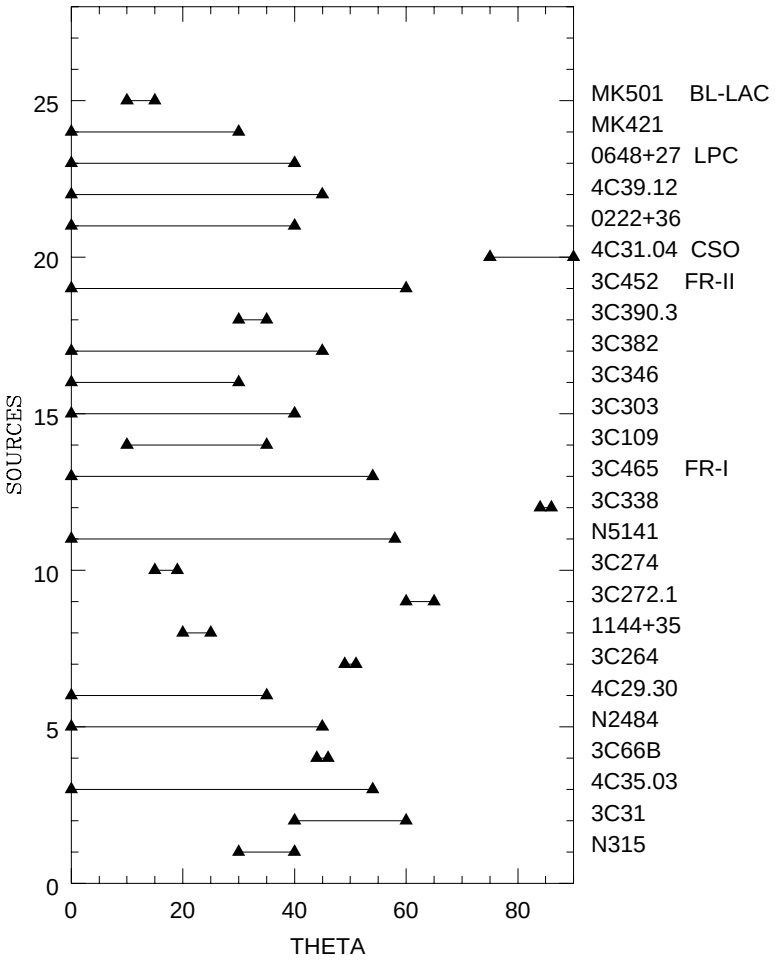

Fig. 3.— Allowed range in the orientation angle θ with respect to the line of sight for different sources. Note that sources are grouped together according to their large scale radio morphology.

1144+35 shows intermediate properties between FR I sources and BL-Lac type objects (Giovannini et al. 1999a) and 3C 274 is a peculiar source (see Sect. 4.4).

Two sources (NGC 315 and 3C 66B) show evidence of an accelerating jet near the core (1 - 5 parsec; see Appendix).

Parsec scale jets are always collimated near the core (with the exception of 3C 274, (Junor et al. 1999)) and appear rather uniform in brightness, with the presence of possible jet substructures at any distance from the core. In 3C 274 it is well known that the jet appears limb-brightened; a similar structure is visible in 1144+35 at about 20 pc from the core (projected). We cannot exclude that a limb-brightened morphology could be present in a larger number of sources, but higher sensitivity and higher resolution data are necessary to reveal it (see Sect. 4.5).

Furthermore, we point out that we are imaging different regions of the parsec scale jets in different sources, given the different redshift and orientation angle of the present sources. Among the 13 FR I radio galaxies, only in three cases we are able to image the jet out to more than 50 pc from the core (de-projected distance): 3C 264, 1144+35, and 3C 274. In 1144+35 and 3C 274 we find evidence of a limb-brightened jet structure in this distant region; in 3C 264 the jet is well collimated and narrow up to $\sim$ 100 pc and it shows a strong widening, filaments and a possible helical structure at a larger distance from the core. At a shorter distance from the core (1 to 50 pc) we have in all cases centrally peaked jets, except 3C 274. In a few cases (see e.g. 3C 66B) there is a sharp change in the jet brightness, but no critical scale was found. Only for a few sources can we obtain images on linear scales smaller than 1 pc. In these cases, we see a collimated, centrally peaked jet with the exception of 3C 274. In this source, an extended jet emission is visible, possibly related to the collimation process. A strong collimation of the jet occurs on apparent scales $\gtrsim$0.04 pc from the central engine (see Junor et al. (1999)).

4.2. FR II Radio Galaxies

Among the FR II sources, one shows a symmetric two-sided structure (3C452) while five have a one-sided jet (3C109, 3C303, 3C346, 3C382, and 3C390.3). This result is in very good agreement with the unified scheme model predictions, because 3C452 the only Narrow Line FR II galaxy in our sample, while other FR II galaxies are well known Broad Line Radio Galaxies. The main jet in the pc scale image is always on the same side with respect to the core as the main kpc scale jet, and the jet position angles are in agreement within a few degrees. This is expected if the jet asymmetry present in FR II radio galaxies is due to the Doppler effect in jets moving at relativistic velocities in the pc and kpc scale.

Comparing parsec scale jets in FR I and FR II sources we note that in our images FR I jets show a uniform brightness when observed with a good uv-coverage, while FR II jets show a structure characterized by the presence of a few blobs. This difference is difficult to quantify and could be related to a difference in the jet properties. We exclude that it could be an effect due to

the *clean* procedure and poor uv-coverage, since the three FR II images presented here for the first time were obtained with an array of 17 telescopes (see Appendix).

No evidence of a larger jet velocity in FR II than in FR I sources is present in our data (see Fig. 2).

4.3. Compact Sources

The compact sources there include two BL-Lac type objects (Mkn 421 and Mkn 501), four Low Power Compact Sources (LPC: 0222+36, 0331+39, 0648+27, and 1217+29), one Compact Symmetric Object (0116+31) and one Compact Steep Spectrum source (0258+35).

The two BL-Lacs show high velocity pc-scale jets oriented at a small angle with respect to the line of sight. In Mkn 421 we see a complex jet with no evidence of a limb-brightened structure whereas in Mkn 501 a limb-brightened jet is well visible at ~ 50 pc from the core (de-projected).

In two LPC sources there is evidence of fast jets oriented at a small angle with respect to the line of sight. In one case (0331+39) the jet is visible for more than 50 pc and could be limb-brightened starting at about 15 pc from the core (de-projected). In 0222+36 no jet was detected, but the core dominance suggests a source orientation at a small angle with respect to the line of sight and some relativistic boosting due to a relativistic jet not visible in our images. The evidence of relativistic jets oriented at a small angle with respect to the line of sight and the absence of an extended structure at arc-second resolution, suggests that these sources could be classified as intermediate or low power BL-Lac sources whose observed core power is too low to dominate the optical emission and therefore are classified as galaxies. We remember that LPC sources do not have a steep radio spectrum.

NGC 4278 shows diffuse emission on a linear scale smaller than 1 pc. All the radio emission is confined within this small size source. No jet like structure is clearly visible and no constraint can be given on the source orientation. More observations are necessary to properly discuss this source.

For the CSO and CSS source we refer to the comments given in the Appendix.

4.4. High Velocity Jets

There are several strong and widely accepted lines of evidences for the existence of relativistic bulk velocities in the parsec scale jets of radio galaxies: the observed super-luminal motions, the rapid variabilities, the observed high brightness temperatures, the absence of strong inverse-Compton emission in the X-ray and the detection of a high frequency emission (gamma ray) for the two BL-Lacs Mkn 421 and 501 all seem to require relativistic bulk speeds with Lorentz factor

$(\gamma) \gtrsim 3$.

The results, discussed in the previous sections, confirm that radio jets move at high velocities on the mas scale. Since in many cases we can only give a lower limit to γ, to better investigate this point we assumed different γ values and we tested if the derived source properties were in agreement with the observational data. Once a jet velocity is assumed, the jet orientation is constrained by the observational data and it is possible to compute the corresponding Doppler factor δ ($\delta = (\gamma(1 - \beta cos\theta))^{-1}$ for each source (in Table 3 we present the estimated orientation angle and Doppler factor ranges assuming $\gamma = 5$). Then, from the value of δ and of the measured radio power, we can derive the intrinsic core radio power for each source: $P_{c-observed} = P_{c-intrinsic} \times \delta^2$ (assuming $\alpha = 0$). In Table 4 we report the intrinsic radio power (assuning $\gamma = 5$), and for a comparison, the observed total and core radio power. Since there is a range of possible jet orientations, we have a possible range of values for δ and therefore of $P_{c-intrinsic}$.

We derived the intrinsic core radio power for different values of γ. In figure 4 we show the total core radio power at 408 MHz versus the intrinsic core radio power at 5 GHz estimated with $\gamma = 5$. Vertical bars represent the possible range of the intrinsic core radio power implied by the estimated range of δ. Despite the large range of possible values allowed in the core dominance (see Sect. 3.2) and the possibility to have low and high power radio sources with a different γ value, we find a small dispersion and a good agreement with the correlation between the observed core radio power and the total core radio power. The line drawn in Fig. 4 is the same line as in Fig. 1 taking into account that now we are plotting the intrinsic core radio power:

$$\log P_{ci5} = 0.62 \log P_t + 8.41$$

where P_{ci5} is the intrinsic core radio power derived assuming $\gamma = 5$. If we compare Figure 1 and Figure 4 we see that the points corresponding to the present sample are in good agreement with the median line and have a small dispersion around it. This is expected, since the dispersion visible in Figure 1 (due to different orientation angles) has been removed, as in Fig. 4 we plotted the intrinsic core radio power. A similar result was obtained for γ in the range 3 - 10. If we assume $\gamma < 3$, the Doppler correction is such that the points corresponding to the present galaxies are not around the best fit line but at a higher value (as in Fig. 1). $\gamma > 10$ implies a higher dispersion of the observed core radio power with respect to the point dispersion found in Giovannini et al. (1988). Present data are in agreement with a γ value in the range 3 - 10. In the future, with a larger sample we could give stronger constraints to the value of γ.

One point in the plots is definitely too low for any γ: the intrinsic core radio power derived for 3C 274 is always lower than the value expected from its total radio power. This source would agree with the correlation displayed in Fig. 4 with a Doppler factor ~ 1, which would imply a jet orientation in the range 35°–40° and not smaller than 19°. Such a value is in contrast with the high super-luminal motion found with optical data (see the discussion in Biretta et al. (1999)) unless a high jet velocity ($\gamma > 12$) is assumed (see Biretta et al. (1999)). Even taking into account that most of the total radio power in 3C 274 at low frequency is due to the large extended halo

Table 3. Jet orientation and Doppler factor with $\gamma = 5$

Name IAU	Name other	Type	θ_5 degree	δ_5
0055+30	NGC 315	Fr I	30 - 40	1.32 - 0.80
0104+32	3C 31	FR I	50 - 60	0.54 - 0.39
0116+31	4C31.04	CSO	75 - 80	0.27 - 0.24
0206+35	4C35.03	FR I	35 - 54	1.01 - 0.47
0220+43	3C66B	FR I	45	0.65
0222+36		LPC	25 - 40	2.13 - 0.80
0258+35	NGC 1167	CSS	—	—
0331+39	4C39.12	LPC	35 - 45	1.01 - 0.65
0410+11	3C 109	FR II	23 - 34	2.04 - 1.07
0648+27		LPC	30 - 40	1.32 - 0.80
0755+37	NGC 2484	FR I	30 - 45	1.32 - 0.65
0836+29	4C29.30	FR I	25 - 35	2.13 - 1.01
1101+38	Mkn 421	BL-Lac	20 - 28	2.52 - 1.48
1142+20	3C 264	FR I	~ 50	0.54
1144+35		FR I	~ 25	1.79
1217+29	NGC 4278	LPC	—	—-
1222+13	3C 272.1	FR I	60 - 65	0.39 - 0.34
1228+12	3C 274	FR I	9 - 10	6
1322+36	NGC 5141	FR I	45 - 58	0.65 - 0.42
1441+52	3C 303	FR II	25 - 40	1.79 - 0.80
1626+39	3C 338	FR I	85	0.22
1641+17	3C 346	FR II	23 - 30	2.04 - 1.32
1652+39	Mkn 501	BL-Lac	10 - 15	5.7 - 3.73
1833+32	3C 382	FR II	35 - 45	1.01 - 0.65
1845+79	3C 390.3	FR II	30 - 35	1.32 - 1.01
2243+39	3C 452	FR II	60 - 70	0.39 - 0.30
2335+26	3C 465	FR I	37 - 54	0.92 - 0.47

Note. — θ_5 and δ_5 are the orientation angle and Doppler factor value assuming $\gamma = 5$.

Table 4. Observed and Intrinsic core radio power

Name IAU	Name other	z	Log P_t W/Hz	Log $P_{c-observ.}$ W/Hz	Log $P_{c-intr5}$ W/Hz	Type
0055+30	NGC315	0.0167	24.56	23.85	23.61 - 24.04	FR-I
0104+32	3C31	0.0169	25.11	23.06	23.60 - 23.88	FR-I
0116+31	4C31.04	0.0592	25.71	23.70	24.84 - 24.94	CSO
0206+35	4C35.03	0.0375	25.46	23.82	23.81 - 24.48	FR-I
0220+43	3C66B	0.0215	25.59	23.56	23.93	FR-I
0222+36		0.0327	24.20	23.76	23.10 - 23.95	LPC
0258+35	NGC1167	0.0160	24.65	$\lesssim$23.43	—	CSS
0331+39	4C39.12	0.0202	24.49	23.42	23.41 - 23.79	LPC
0410+11	3C109.0	0.3056	27.78	26.05	25.43 - 25.99	FR-II
0648+27		0.0409	24.31	24.19	23.95 - 24.38	LPC
0755+37	NGC2484	0.0413	25.65	24.16	23.92 - 24.53	FR-I
0836+29	4C29.30	0.0790	25.70	24.63	23.97 - 24.62	FR-I
1101+38	Mkn 421	0.0300	24.66	24.40	23.60 - 24.06	BL-Lac
1142+20	3C264	0.0206	25.46	23.57	24.11	FR-I
1144+35		0.0630	24.95	24.90	24.39	FR-I
1217+29	NGC4278	0.0021	21.44	$\lesssim$21.08	—	LPC
1222+13	3C272.1	0.0037	23.27	22.03	22.85 - 22.97	FR-I
1228+12	3C274	0.0037	25.07	23.37	21.81	FR-I
1322+36	NGC5141	0.0175	24.36	23.30	23.67 - 24.05	FR-I
1441+52	3C303	0.1410	26.74	25.22	24.71 - 25.41	FR-II
1626+39	3C338	0.0303	25.86	23.62	24.94	FR-I
1641+17	3C346	0.1620	26.98	25.43	24.81 - 25.19	FR-II
1652+39	Mkn 501	0.0337	24.96	24.79	23.28 - 23.65	BL-Lac
1833+32	3C382	0.0586	26.31	24.46	24.45 - 24.83	FR-II
1845+79	3C390.3	0.0569	26.58	24.67	24.43 - 24.66	FR-II
2243+39	3C452.0	0.0811	26.92	24.58	25.63 - 25.40	FR-II
2335+26	3C465	0.0301	25.91	23.99	24.06 - 24.65	FR-I

Note. — Log P_t is the logarithm of the total radio power at 408 MHz. Log $P_{c-observ.}$ and Log $P_{c-intr5}$ are the logarithm of observed and intrinsic core radio power at 5 GHz, with $\gamma = 5$.

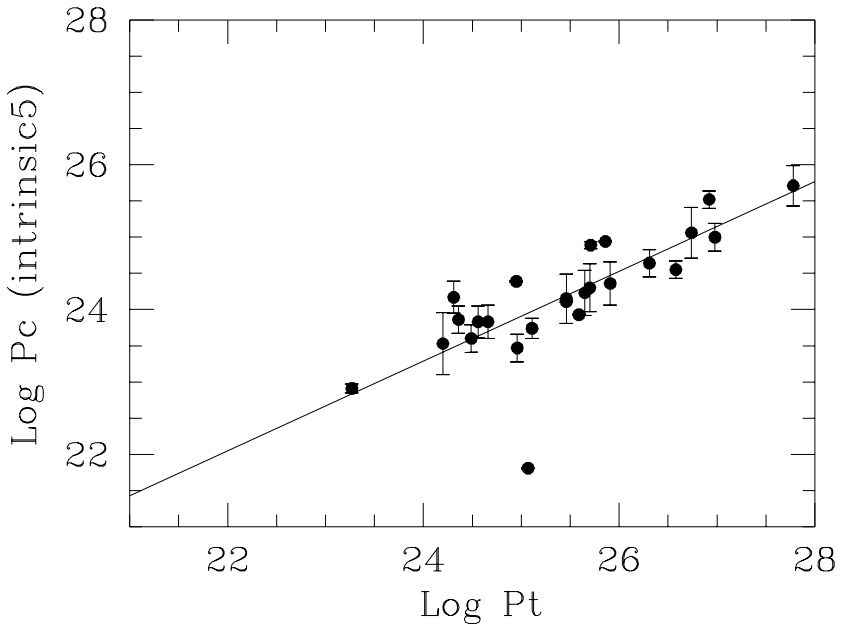

Fig. 4.— Correlation between the core intrinsic radio power and the total radio power. The line is not the best fit but the scaled correlation found between the observed core radio power and the total radio power. $\gamma = 5$ has been assumed. The discrepant point corresponds to 3C274.

emission, whose origin and relation with the core radio power is poorly understood (see Owen et al. (1999) and Harris et al. (1999)), and that therefore the total radio power to be used in the correlation should be probably much lower, the large discrepancy between 3C 274 and the other sources persists. We conclude that 3C274 looks peculiar with respect to the other sources of this sample.

We note that all sources in our sample are in agreement with the same P_c – P_{tot} correlation, despite the variety of their large scale morphology (FR I, FR II, BL-Lacs, and so on). Moreover the correlation holds over 5 orders of magnitude in P_{tot} (see Fig. 4). This result confirms that the properties of parsec scale jets are similar in sources with different total radio power and kpc scale morphology.

A correlation between the core and the total radio power can be expected from simple considerations if the sources are in energy equipartition conditions. In this case the total energy (U_l) in the radio source lobes is:

$$U_l \propto P_l^{4/7} \times V^{3/7}$$

(Pacholczyk 1970) where V is the source volume and P_l is the lobe radio power.

Assuming that the global energy is proportional to the energy carried out by the jets and that the lobe radio power is the total radio power at 408 MHz, we can derive that:

$$P_c \propto P_t^{4/7} \times V^{3/7}/t$$

Where t is the radio source age. The result, $P_c \propto P_t^{0.57}$, is very similar to the slope computed from the core – total radio power correlation (0.62). The time dependence is too low to be relevant if we take into account that the source volume is proportional to t^a with $a \sim 3$ resulting in a final time dependence of $t^{2/7}$ and that most of the sources used to derive the correlation between the core and total radio power are old sources. The small dispersion found and the estimated correlation persists if sources are not too far from the equipartition condition.

4.5. Kiloparsec and Parsec Scale Morphology

The differences in the kpc scale between FR I and FR II sources are well known and established. The most relevant difference related to the present discussion is the evidence that kpc scale jets in FR II sources are still relativistic or mildly relativistic up to the hot spot region, while kpc scale jets in FR I sources are strongly decelerated and become sub-relativistic within 1 - 5 kpc from the core, with typical velocities of a few thousands km/sec.

In this paper we show that parsec scale jets are highly relativistic in FR I and FR II sources. Therefore the difference between FR I and FR II sources on the kpc scale are not related to the parsec scale velocity, but to a larger scale effect. Two different scenarios can be considered:

a) FR II sources have a higher intrinsic jet power which can maintain relativistic jets up to

the hot spot region;

b) FR I sources have a higher density interstellar medium which decelerates the jets.

The first case implies a correlation between the total or core radio power of FR II sources and the jet velocity, and therefore jets in FR I should have on average a lower γ value. This is not the case from present results, where no difference in the jet velocity has been found in FR I and in FR II sources. Moreover the correlation between the core and total radio power does not show any difference among FR I and FR II sources. If FR II sources have higher velocity jets we should see some discontinuity in the core-radio power correlation going from low to high powers.

If the interstellar medium (ISM) in FR I is denser than in FR II, we should see: i) lower polarized flux and higher rotation measure in FR I than in FR II, if the ISM is ionized. In NGC 315 (Cotton et al. 1999) found a very deep limit in the polarized flux density, but data are missing for a comparison between FR I and FR II sources. ii) FR I jets should show a more prominent limb-brightening structure with respect to FR II sources because of a larger interaction with the surrounding medium. As discussed in the next sub-section, the few sources with an evident limb-brightened jet structure on the parsec scale are low power (FR I) radio galaxies or BL-Lac type sources.

In conclusion, our results do not support the idea that large scale differences between FR I and FR II sources are due to intrinsically more powerful and faster parsec scale jets in FR II sources. There is evidence that the jet velocity in FR I sources slowly, but continuously, decreases because of the jet interaction with a dense ISM, and becomes sub–relativistic on the kpc scale.

4.6. Two Velocity Jets?

Chiaberge et al. (2000) derive that a structure in the jet velocity field, with a fast spine surrounded by a slow velocity layer, is necessary to account for the discrepancies among observational data for FR I radio galaxies and BL-Lac objects. A two-velocity jet model was developed by Laing (1996) and supported by observational evidence in some FR I sources. In a two velocity jet, seen at a significant angle to the jet, the emission from the inner portion of the jet is strongly de-boosted, making it weak to invisible. In contrast, the outer, slower portions of the jet have lower Doppler de-boosting and therefore may appear brighter. Such a jet if observed at proper resolution, would appear as a hollow cone, i.e. limb-brightened.

In our sample a limb-brightened structure is clearly present in 3C 274, 1144+35 and Mkn 501 and could be present in 0331+39. We note that the detection of such structure may not be easy: it should be well visible in polarized images (see Aaron (1999) for Mkn 501) which are difficult to obtain because of the low percentage of polarized flux (see e.g. Cotton et al. (1999)), while good angular resolution and high sensitivity are needed in total intensity images. Moreover to distinguish the two velocity regions a critical orientation is crucial to have the low velocity external

region brighter because of Doppler beaming and the inner fast region fainter because it is de-boosted. This is the case of 1144+35 and MKn 501. We also note that the two velocity structure is not visible at the jet beginning, but at some distance from the core. We interpret this as evidence of the presence of an interaction between the jet and the external medium, i.e. the outer layer velocity decreases because of the interaction with the surrounding medium, and this deceleration becomes significant at some distance from the core. The de-projected distance, where the shear layer is visible, is about 50 pc for 1144+35 and Mkn 501, and 20–30 pc for 0331+39, where it could be present. This suggests that jet imaging in the sub-arcsecond scale (i.e. 50 – 100 pc) is likely to be best suited for the detection of limb-brightened structures. Most of our images can track the milliarcsecond jets only out to a few parsecs and only for Mkn 421 and 3C 264 high quality images from a few pc to hundreds of parsecs are available, with no evidence for limb-brightening. Both sources have a complex morphology because of projection effects and jet sub-structures. We conclude that a two–velocity structure in parsec scale jets is present in a few sources, but with the available data we cannot confirm if this kind of structure is present in all sources or only in some of them because of different jet interactions with the surrounding medium. Future observations with the extended VLA will solve this point.

5. Conclusions

In this paper we presented new images at parsec resolution for 10 galaxies (see Appendix), and maps at different frequencies for 2 more sources. Thanks to these new data at least one high quality image at parsec resolution is available for all the sources of our sample.

FR I radio sources are characterized by the presence of highly relativistic parsec scale jets, whose orientation with respect to the line of sight, is in agreement with the predictions of unified scheme models. FR II sources have a radio morphology very similar to FR I radio galaxies and jet velocities are in the same range. A new symmetric two-sided jet was found in the narrow line FR II radio galaxy 3C 452. LPC sources show relativistic jets at a small angle to the line of sight. We suggest that most of LPC sources are intermediate BL-Lacs where the observed nuclear emission is too faint to be dominant with respect to the parent galaxy radiation because of the intermediate jet orientation angle and/or the faint nuclear power.

Assuming different jet velocities, we derived the corresponding intrinsic core radio power, and we correlated it with the low frequency total radio power. We found that the core to total radio power ratio is in very good agreement with the correlation derived from the analysis of B2 and 3CR catalogs assuming a jet bulk speed in the range $\gamma = 3 - 10$. The dispersion around the best fit is small as expected since we have removed the differences due to the orientation angle. This result confirms that sources with different kpc scale morphology and radio power, are similar on the parsec scale. The slope of the correlation is in agreement with the expected value from equipartition conditions.

The similarity of radio morphology and jet velocity on the parsec scale is in contrast with the large difference on the kpc scale between high and low power radio sources. We briefly discussed the reason of this difference, and suggested that it could be due to a denser ISM in low power radio sources. A strong interaction between the relativistic jet and the surrounding medium can produce a decrease of the jet velocity and therefore FR I jets will become sub-relativistic after a few hundreds of parsecs and sub–relativistic within a few kiloparsecs. Conversely, jets in FR II sources are mildly relativistic up to the hot spot region. A systematic higher γ value in FR II sources is excluded by the present data.

A decrease in the jet velocity in low power sources should give rise to different morphological properties in parsec scale images. One major difference could be the presence of a two velocity regime in low power source jets responsible of the limb-brightened structures. We discussed the difficulty to image such jet structure and we noted that the few sources with a limb-brightened structure are low power sources. This could be evidence of the interaction between the jet and the ISM producing a jet deceleration in low power sources.

The authors wish to thank R. Fanti for helpful suggestions and discussions, and G. Taylor for a critical reading of the manuscript. We thank the staff of NRAO and EVN telescopes involved in the observations, for their help. NRAO is a facility of the National Science Foundation, operated under cooperative agreement by Associated Universities, Inc. This work was partly supported by the Italian Ministry for University and Research (MURST) under grant Cofin98-02-32. GG, LF, and TV acknowledge partial financial support from the European Commission TMR Programme, Access to Large-Scale Facilities under contract ERBFMGECT950012. This research has made use of the NASA/IPAC Extragalactic Data Base (NED) which is operated by the JPL, California Institute of Technology, under contract with the Natonal Aeronautics and Space Administration.

A. Observations and Data Reduction

The observational details for each source are given in Table 5: source names (Col. 1 and 2); observing array (Col. 3); observing frequency, time (Col. 4 and 5) and observing date (Col. 6). The observations of the sources 0222+36 (on 97–02–22) and 3C 272.1 were correlated in Bonn, all other observations have been correlated in Socorro (NM).

Post correlation processing used the NRAO AIPS package. Amplitude calibration was initially done using standard method employing measured system temperatures and assuming sensitivity calibration and refined using compact calibrator sources. Phase calibration was done using strong calibrator sources observed during the scheduled time. All data were globally fringe fitted (Schwab & Cotton 1983) and then self–calibrated. No polarization information is available.

B. Notes on Individual Sources

0055+30 – NGC315 In previous papers (Cotton et al. (1999) and ref. therein) we published multi–frequency and multi–epoch data on this giant radio galaxy. We found evidence of an acceleration in the inner parsec scale jet. A similar result was presented by Lobanov & Zensus (1999) for the well known quasar 3C 345, by Sudou et al. (2000) for NGC 6251, by Homan et al. (2000) in the jet of 5 Blazers from proper motion observations and here for the source 0220+43 (3C66B). Barth et al. (1999) reported the detection in NGC 315 of a polarized broad Hα emission.

0104+32 – 3C31 Observations at 6 cm were published in Lara et al. (1997).

0116+31 – 4C31.04 In a previous paper Cotton et al. (1995) suggested that this source could be a low redshift Compact Symmetric Object (CSO). Conway (1996) showed the presence of a complex HI absorption across both lobes.

We observed this source with the VLBA and one single VLA telescope for 4 hours at 5 GHz on July 1995. In Fig. 5 we present an image obtained with these new data. A comparison with the images published by Cotton et al. (1995), confirms the reality of the faint component in between the two extended lobes and its identification as the core source. Its spectrum is flat, its flux density being 14 mJy at 8.4 GHz and 14.5 mJy at 5 GHz. The spectral index of the East lobe is $\alpha_5^{1.7} = 0.5$ and $\alpha_{8.4}^{5} = 0.8$; in the W lobe is $\alpha_5^{1.7} = 0.5$ and $\alpha_{8.4}^{5} = 1.5$ (we note however that we could have missing flux problems at 8.4 GHz as discussed in Cotton et al. (1995)). This result confirms the identification of 0116+31 (4C31.04) as a nearby CSO source.

No jet-like structure is visible on either side of the core even if both lobes show an elongated emission in between the region with the highest brightness in the lobes and the core. The symmetric structure and the core to total radio power ratio suggests that this source is near to the plane of the sky ($\theta \gtrsim 75^\circ$). This result is in agreement with the Conway (1996) model and explains the lack of visible jets, since at this orientation relativistic jets are strongly de-boosted.

Table 5. The new observations

Name IAU	Name other	Stations	Frequency GHz	Time hours	Date yy-mm-dd
0116+31	4C31.04	VLBA Y1	5.0	4	95-07-22
0220+43	3C66B	VLBA Y27 GB EB JB MC NT ON	5.0	6	93-09-12
0222+36		VLBA Y1	5.0	4	95-07-22
		EB MC NT ON JB TR	5.0	2	97-02-22
0258+35	NGC1167	VLBA Y27 GB EB JB MC NT ON	5.0	6	93-09-12
0331+39	4C39.12	VLBA Y1	5.0	4	95-07-22
0648+27		VLBA Y1	5.0	4	95-07-22
1217+29	NGC4278	VLBA Y1	5.0	4	95-07-22
1222+13	3C272.1	BR FD HN LA PT SC JB MC NT	1.7	10	96-02-10
1322+36	NGC5141	VLBA Y27 GB EB JB MC NT ON	5.0	6	93-09-12
1441+52	3C303	VLBA Y1 EB CM MC NT ON TR	5.0	4	97-09-23
1833+32	3C382	VLBA Y1 EB CM MC NT ON TR	5.0	4	97-09-23
2243+39	3C452.0	VLBA Y1 EB CM MC NT ON TR	5.0	4	97-09-23

Note. — Stations: VLBA = full VLBA (10 telescopes); BR = VLBA-Brewster; FD = VLBA-Fort Davis; HN = VLBA-Hancock; LA = VLBA-Los Alamos; PT = VLBA-Pie Town; SC = VLBA-Saint Croix; NL = VLBA-North Liberty; Y27 = VLA phased array; Y1 = VLA single antenna; GB = Green Bank (NRAO); EB = Effelsberg; CM = Cambridge; MC = Medicina; JB = Jodrell Bank; NT = Noto; ON = Onsala; TR = Torun; WS = Westerbork

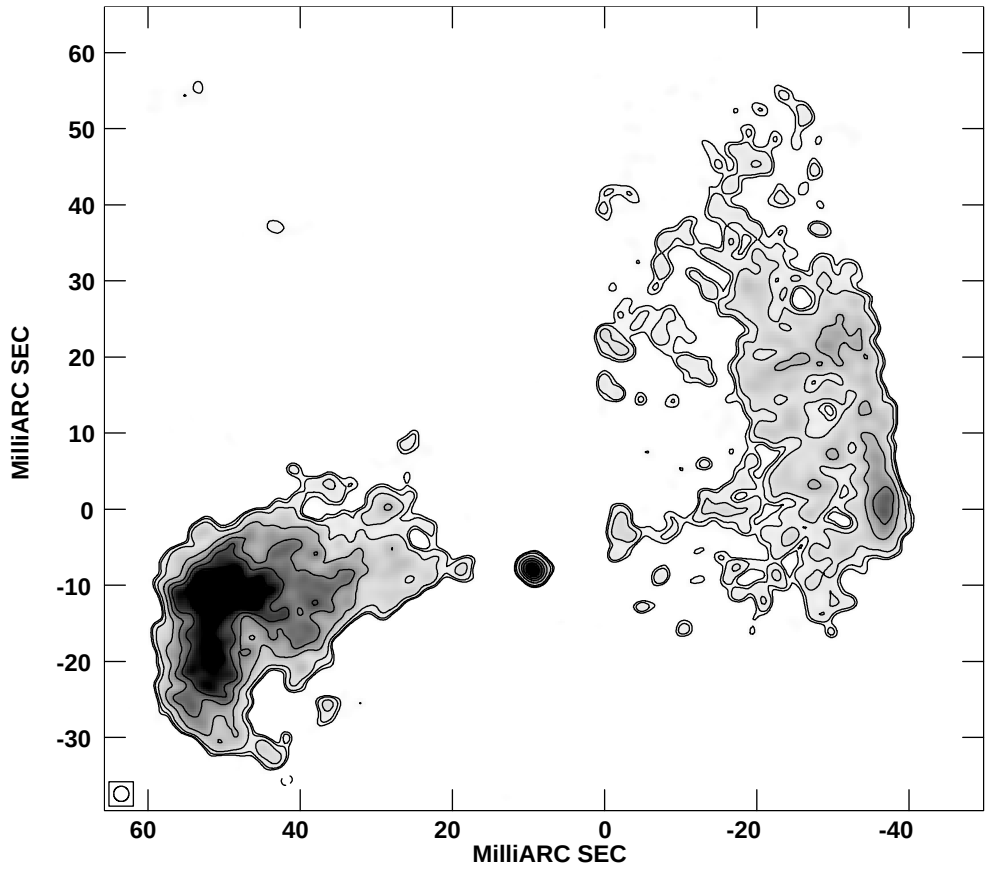

Fig. 5.— VLBA image at 5 GHz of 0116+31 (4C31.04). The HPBW is 2 mas. The noise level is 0.2 mJy/beam and levels are: -1, 0.8, 1, 1.5, 3, 7, 7, 10, 15 and 20 mJy/beam. The peak flux density is 20.6 mJy/beam.

0206+35 − 4C35.03 Observations at 5 GHz have been published in Lara et al. (1997).

0220+43 − 3C66B This radio galaxy is characterized by the presence of an optical and infrared jet (see Jackson et al. (1993) and Tansley et al. (2000)). At arc-second resolution it was studied in detail by Hardcastle et al. (1996). These authors report also evidence of radio nuclear flux density variability and studied the kpc scale jet asymmetry. A possible optical emission from the counter-jet was reported by Fraix-Burnet (1997).

We observed this source with global VLBI at 6 cm. The uniform weight map is presented in Figure 6. The image shows the main jet emission visible up to 20-25 mas from the core. At higher resolution, a faint counter-jet is visible (Fig. 7). We checked accurately the reality of this faint counter-jet emission, and unsuccessfully tried to eliminate it from the image. Thanks to the very good uv coverage of our data we are confident that this structure is real. The jet/counter-jet ratio at 1.5 - 2 mas from the core is ~ 10 which corresponds to $\beta \cos\theta \sim 0.43$. At larger distance ($\sim 5$ mas) the jet/counter-jet ratio increases up to R $\gtrsim$100 implying a small angle with respect to the line of sight. Taking into account the core dominance we derive a jet orientation $\theta \sim 45^\circ$ and a jet velocity $\beta \sim 0.6$ at 1.5 mas from the core and ~ 0.99 at 4-5 mas from the core. This result is very similar to that obtained by us for NGC 315 and by Sudou et al. (2000) for NGC 6251 and in agreement with Lobanov & Zensus (1999) for 3C345.

A high jet speed could explain the presence of the gap between the mas and the arc-second scale, a high velocity jet being de-boosted. In the region of the bright optical jet, we need $\gamma \leq 2$, to avoid de-boosting effects, in agreement with Tansley et al. (2000).

We note that these values are in agreement with the result $\theta \lesssim 53^\circ$ estimated by Hardcastle et al. (1996) on the kpc scale.

0222+36 This source shows a halo-core structure at arc-second resolution (Fanti et al. 1987). The spectral index between 408 and 5000 MHz is straight and moderately flat ($\alpha_{0.4}^{5.0} = 0.4$). We observed this galaxy with the EVN array at 5 GHz on February 1997 and with the VLBA on July 1995. In both observations, we detected an unresolved source with a total flux density comparable to the arc-second core flux density. From the core to total power ratio we derive that this source should be oriented at an angle to the line of sight smaller than 40°.

0258+35 − NGC1167 This source was studied with VLA and MERLIN+EVN observations at 1.6 GHz by Sanghera et al. (1995) who classified it as a CSS source. VLA data show a double structure with a separation of 1.1". In the EVN+MERLIN images it reveals an extended plume-like feature at both ends of the source and a jet-like feature in between. Due to the complex structure the core identification is not obvious.

We observed this source with global VLBI observations at 5 GHz. The source is marginally detected at the longest baselines but it shows a large increase in the correlated flux density on the shortest baselines as EB-JB (in the EVN) and Y27-PT-LA (in the US). Our final image shows a core-jet structure (Fig. 8), however the large difference between this high resolution map and the

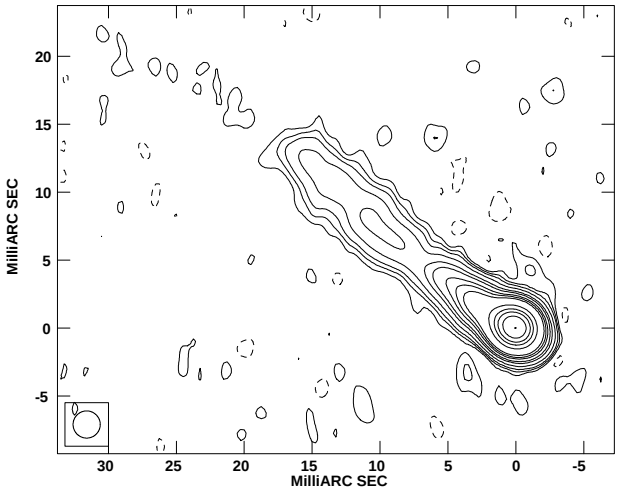

Fig. 6.— Global VLBI image of 0220+43 (3C66B) at 5 GHz. The HPBW is 2 mas. The noise level is 0.06 mJy/beam and levels are: -0.15, 0.15, 0.3, 0.5, 1, 2, 3, 5, 7, 10, 30, 50, 70, 100 and 150 mJy/beam.

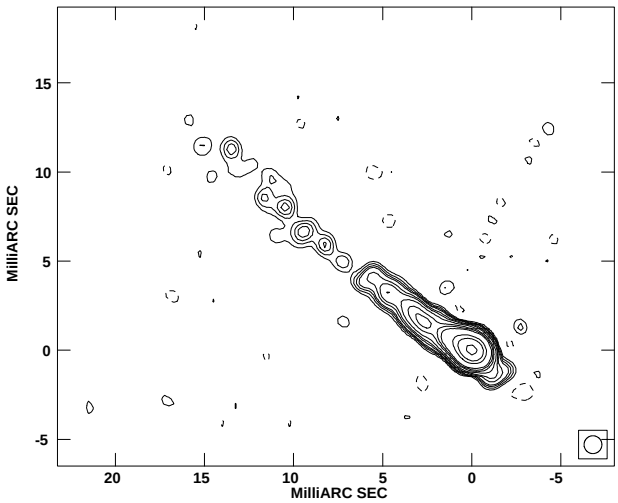

Fig. 7.— As Figure 6 but at full resolution: HPBW = 1 mas. The noise level is 0.1 mJy/beam and levels are: -0.4, 0.4, 0.6, 0.8, 1, 1.5, 2, 3, 5, 7, 10, 30, 50 and 100 mJy/beam.

MERLIN+EVN image at 1.6 GHz by Sanghera et al. (1995), does not allow us to properly identify the nuclear source, even if our extension is in the same direction of the jet-like feature visible in the EVN+MERLIN image. The peak flux in our image is 26.3 mJy/beam and the total flux density is 34 mJy. We note that in our shortest baseline (Y-PT) a correlated flux of $\sim$ 170 mJy is visible confirming the diffuse morphology of the extended structure visible in the MERLIN images and its steep spectrum.

More observations with shorter baselines are necessary to properly study this source.

0331+39 − 4C39.12 We observed this source with the VLBA and one single VLA telescope for 4 hours at 5 GHz on July 1995. The source shows an one-sided structure at the same PA as the short extension visible in the VLA map at 5 GHz (Fanti et al. 1986). The parsec scale jet is straight in the inner 12 mas after which it becomes transversely resolved with many substructures possibly due to a helical structure although we cannot exclude a limb-brightened structure (Figure 9 and 10).

The limit on the jet/counter jet ratio is not very high because of the jet low brightness ($R \gtrsim 12$) therefore the major constraints on the jet orientation and velocity were derived from the core dominance, which gives θ lower than 45°. A small angle with respect to the line of sight is in agreement with the halo-core structure of the radio emission at arc-second resolution.

3C109 We published VLBI and VLA observations of this FR II Broad Line Radio Galaxy (BLRG) in Giovannini et al. (1994).

0648+27 This source is unresolved at arc-second resolution and has a spectral index $\alpha_{0.4}^{5.0} = 0.6$ suggesting the existence of a radio structure in the mas or sub-arcsecond scale. The measured flux densities at arc-second resolution are: S_{408} 270 mJy, S_{1415} 156 mJy (Fanti et al. 1987) and S_{5000} 58 mJy (Gregory & Condon 1991), while Antonucci (1985) reports a flux density of 213 mJy with VLA B array observations at 5 GHz.

We observed this galaxy with VLBA + Y1 at 5 GHz on July 1995 and found an unresolved core with a flux density of 47 mJy and a faint one-sided emission extended 20 mas with a variable direction (Fig. 11). From this asymmetric structure and the core dominance we derive that this source is oriented at $\theta \lesssim 40°$ with a jet velocity $\gtrsim 0.7c$.

0755+37 − NGC2484 We published VLBI and VLA observations of this FR I Radio Galaxy in Giovannini et al. (1994).

0836+29 − 4C29.30 We published VLBI and VLA observations of this FR I Radio Galaxy obtained on November 1990, in Venturi et al. (1995). A second epoch observation always at 6 cm was obtained on May 1994. A comparison of the two images does not reveal any proper motion. More efforts, as in NGC 315, are necessary to measure a possible proper motion in this source.

1101+38 − Mkn 421 This BL-Lac source was studied in detail by Piner et al. (1999). We presented a VLBA image in Giovannini et al. (1999b) and a more detailed paper is in preparation.

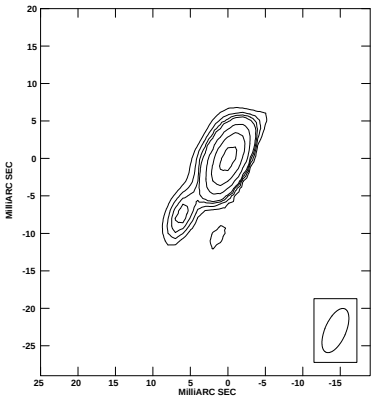

Fig. 8.— Global VLBI image of 0258+35 (NGC1167) at 5 GHz. The HPBW is 6.3 × 2.8 mas (PA = -23°). The noise level is 0.2 mJy/beam and levels are: -1, 1, 1.5, 2, 2.5, 5, 10 and 20 mJy/beam.

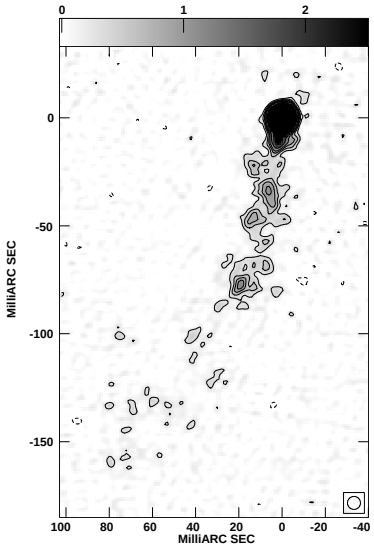

Fig. 9.— VLBA image of 0331+39 with natural weight at 5 GHz. The HPBW is 6 mas. The noise level is 0.08 mJy/beam and levels are: -0.25, 0.25, 0.5, 0.75, 1, 1.5, 3, 5, 10, 20, 30, 50, 70 and 100 mJy/beam.

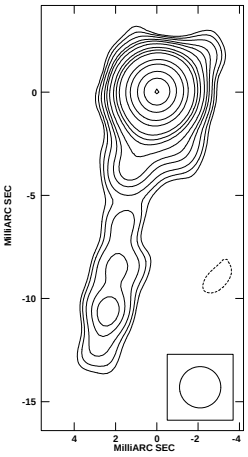

Fig. 10.— VLBA image of 0331+39 at 5 GHz with uniform weight: HPBW = 2 mas. The noise level is 0.15 mJy/beam and levels are: -0.5, 0.5, 0.7, 1, 1.5, 2, 3, 5, 7, 10, 20, 30, 50, 70 and 90 mJy/beam.

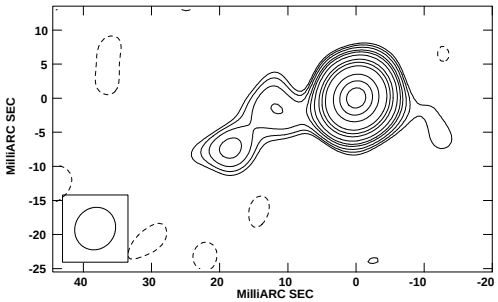

Fig. 11.— VLBA image of 0648+27 at 5 GHz. The HPBW is 6.4 × 5.9 mas (PA -30°). The noise level is 0.2 mJy/beam and levels are: -0.5, 0.5, 0.7, 1, 1.5, 2, 3, 5, 7, 10, 20, 30 and 40 mJy/beam.

The core dominance for this source is low (to be a BL-Lac) even if we take into account the core variability (Piner et al. 1999). The presence of proper motion is uncertain: from our data we derive a possible proper motion of $\sim$ 1.5 c (Giovannini et al., in preparation), while Piner et al. (1999) found sub luminal proper motions (or no motion at all) and Marscher (1999) found a proper motion with an apparent velocity of the order 2-3 c.

Taking into account the jet/counterjet ratio and the core dominance, we can have: a) a high velocity jet but in this case the angle with respect to the line of sight should be near 20°; b) a jet oriented at a small angle ($\sim 5°$) with β as low as 0.9. In either cases we have a low Doppler factor. If we want to reconcile this result with the high Doppler factor requested by gamma ray and variable emission, we need a) a large change in the jet orientation from the TEV to the radio emission region; or b) a large decrease of the jet velocity from the TEV to the radio emission region. Given the radio morphology of the pc scale jet with its diffuse emission, both cases (a) and (b) are probably present.

1142+20 - 3C264 We discussed the properties of this source in Lara et al. (1997), Baum et al. (1997), Lara et al. (1999) and Lara et al., in preparation. We assume here as jet dynamics the results given in Baum et al. (1997). This source is classified as a low luminosity BL Lac by Rector et al. (1999).

1144+35 See Giovannini et al. (1999a) for a detailed discussion on this superluminal source.

1217+29 − NGC 4278 This nearby (z = 0.0021; distance modulus = 30.61, corresponding to 13.2 Mpc) elliptical galaxy shows strong nuclear optical emission lines and a large amount of neutral hydrogen (see Schilizzi et al. (1983) and references therein). At arc-second resolution it shows an unresolved emission, while an extended structure is visible at mas resolution (Schilizzi et al. 1983).

We observed this source with VLBA + Y1 on July 1995 at 5 GHz. Our image (see Figure 12) shows a complex structure with a central emission with a peak flux density of 95 mJy/beam and an extended halo which at North shows a large bend, being oriented E-W in the external regions. A distorted jet-like structure could be present in the southern region, however due to the extended structure also in the northern region, no information on the jet velocity and orientation may be derived from present data. Our image is in good agreement with the map presented by Schilizzi et al. (1983) at a lower angular resolution and with the image given by Falcke et al. (2000) where only the southern jet like structure is visible because of their lower sensitivity to extended structures (they do not have the short baseline VLA - VLBA Pt). A comparison with unpublished images at 8.4 GHz by us, confirms the core identification with the central region where the highest brightness is measured. The VLBI total flux density is $\sim$ 400 mJy in agreement with arc-second scale observations, therefore we are confident to have mapped the whole structure of this small size source. We note that due to the nearness of this source the linear resolution of our image is very good (the HPBW is 2.5 mas corresponding to 0.15 pc).

1222+13 − 3C272.1 A preliminary map of this source at 5 GHz presented in Giovannini et

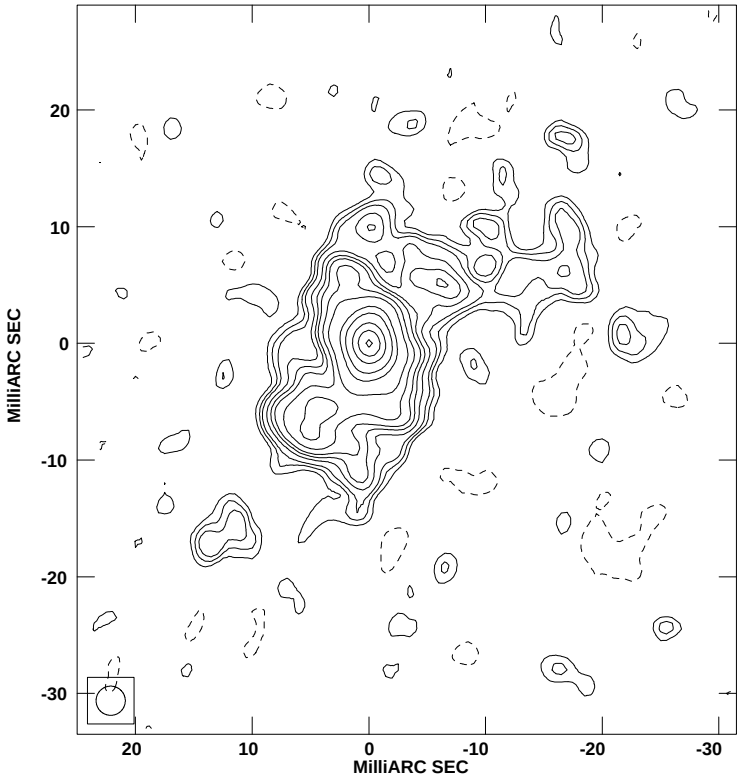

Fig. 12.— VLBA image of 1217+29 (NGC4278) at 5 GHz. The HPBW is 2.5 mas. The noise level is 0.4 mJy/beam and levels are: -1, 1, 1.5, 2, 3, 4, 5, 7, 10, 20, 30, 50, 70, and 90 mJy/beam.

al. (1995) suggested a possible two-sided structure. We present now a new better image obtained at 1.7 GHz where this nearby source shows a clear one-sided structure (Fig. 13). A new reduction of previous 5 GHz data confirms the one-sidedness of this source. The main problem in the 5 GHz data is the poor uv-coverage with large gaps and the relatively faintness of the extended emission. The present image is in agreement with results obtained in different observations using the full VLBA by Xu et al. (2000).

From the present data, we derived a limit on the ratio between the jet and counter-jet $>_{\sim}10$ which implies $\theta \lesssim 65°$. The low core radio power suggests that it is strongly de-boosted and therefore at a large angle with respect to the line of sight. We derive that θ has to be $\gtrsim 60°$. Taking into account both constraints we estimate $\theta \sim 60°$ - $65°$ with $\beta \gtrsim 0.9$. This result is in agreement with the asymmetry visible at the beginning of the arc-second jet (see the unpublished image by Laing and Bridle in *An Atlas of DRAGNs* - http://www.jb.man.ac.uk/atlas/) and with the gap of radio emission in the sub-arcsecond scale.

1228+12 – 3C274 This source is well studied at all frequencies and angular resolutions. See e.g. Junor et al. (1999), Biretta et al. (1999) and references in.

1322+36 – NGC5141 We observed this small size FR I radio galaxy for 6 hours at 5 GHz on September 1993. The final image shows an one-sided jet emission extended $\sim$ 10 mas in the same direction of the main large scale jet (Fig. 14).

We derive a jet/counter-jet ratio > 20 which gives a value of $\beta cos\theta > 0.54$ implying a jet velocity $\beta \gtrsim 0.54$ and an orientation angle $\theta \lesssim 58°$.

1441+52 – 3C303 This Broad Line Radio Galaxy shows an extended structure at arc-second resolution, two hot spots and a prominent one-sided jet (Leahy and Perley 1991). We have observed this source with a global array of 17 telescopes for 6 hrs at 5 GHz. Our final map is in Fig. 15. The parsec scale image shows an one-sided jet in the same orientation of the arc-second scale jet. In the inner 5 mas, the radio emission is not resolved transversely while in the 5 - 15 mas region the jet emission becomes fainter and oscillating.

From the jet sidedness and the core prominence we derive that the radio emission is oriented at an angle $\theta \lesssim 40°$ and the jet velocity has to be $\gtrsim$0.7c. The derived jet orientation and velocity is in agreement with the presence of broad lines in the optical spectrum and with the arc-second radio structure.

1626+39 – 3C338 We are monitoring this source because of its two-sided structure and measured proper motion. Our last paper on this source is Giovannini et al. (1998a).

1641+17 – 3C346 See Cotton et al. (1995) for a discussion on the parsec scale structure of this Broad Line Radio Galaxy.

1652+39 – Mkn 501 We observed this source also with the space VLBI array. Preliminary results have been published in Giovannini et al. (1999b) and Giovannini et al. (1998b). A more

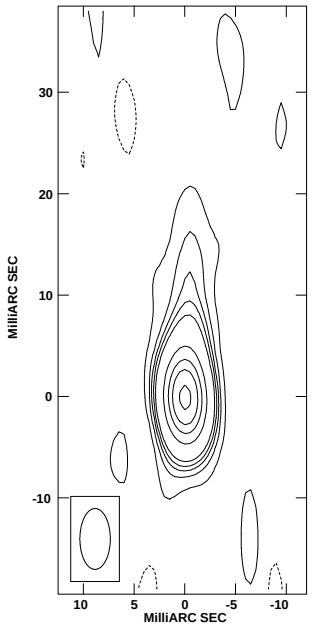

Fig. 13.— Global VLBI image of 1222+13 (3C272.1) at 1.7 GHz. The HPBW is 6 × 3 mas in PA 0°. The noise level is 0.5 mJy/beam and levels are: -1, 1, 3, 5, 7, 10, 30, 50, 70, and 100 mJy/beam.

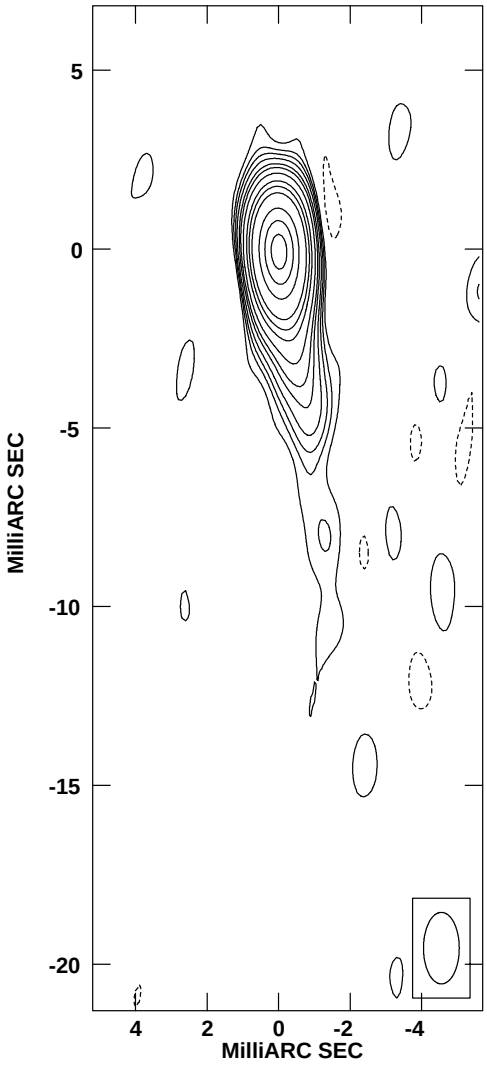

Fig. 14.— Global VLBI image of 1322+36 (NGC5141) at 5 GHz. The HPBW is 2 × 1 mas in PA 0°. The noise level is 0.14 mJy/beam and levels are: -0.3, 0.3, 0.5, 0.7, 1, 1.5, 2, 3, 5, 7, 10, 20, 30, and 40 mJy/beam.

detailed paper is in preparation.

1833+32 − 3C382 An 8.4 GHz VLBI image of this source was published in Giovannini et al. (1994). We present here new observations with a global array of 17 telescopes for 6 hrs at 5 GHz. The new image is in good agreement with the old one. Thanks to the better sensitivity and uv coverage we see a more extended jet with a peak brightness at its end (Fig. 16). The possible change in the jet PA near the core is not confirmed by the new data. A comparison of the 8.4 and 5 GHz images shows some displacement between local peaks possibly due to proper motion, but the large epoch difference and the very different uv coverage (and frequency) does not allow us to estimate it.

1845+79 − 3C390.3 This super-luminal Broad Line Radio Galaxy has been studied by Alef et al. (1996). They suggest a proper motion with an apparent velocity of 3.5 c. Taking into account this result and the core dominance (the main jet is faint, therefore no strong constraint can be derived from the jet sidedness) we derive that θ is in the range 30-35 degree with $\beta \sim 0.96$ - 0.99. The derived low Doppler factor is in agreement with the faint pc scale jet. The value of θ is in agreement with the kpc scale structure and the presence of broad lines in the nuclear region.

2243+39 − 3C452 We have observed this FR II narrow line and symmetric radio galaxy with a global array of 17 telescopes for 6 hrs at 5 GHz. The parsec scale images show a very symmetric structure (Fig. 17). We identify the core source as the central peak taking into account also the symmetric kpc scale structure, but new observations at different frequencies are necessary to confirm this result. The pc scale jet position angle (90°) in the inner 5 mas from the core is slightly different from the kpc scale one ($\sim 75°$). However in a lower resolution image (Fig. 18) a low surface brightness is visible up to 20 mas from the core possibly oriented as the kpc scale structure. The pc scale jet brightness shows two different regions: it is high up to ~ 5 mas from the core and shows a strong decrease at larger distances. From the jet symmetry and the core dominance we derive that this source should be oriented at $\theta \gtrsim 60°$.

2335+26 − 3C465 This extended WAT source was studied in Venturi et al. (1995). A second epoch global observation obtained on September 1993 at 8.4 GHz (not shown here) does not reveal any visible proper motion, because of the short time range and of the uniform brightness of the parsec scale jet. More effort is necessary to measure a possible proper motion in this source.

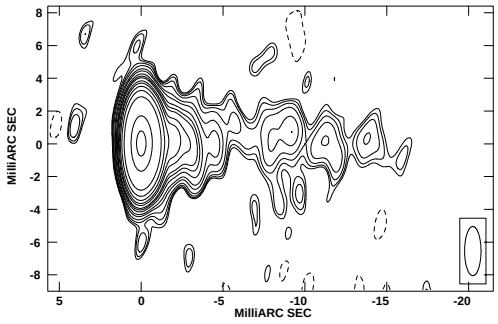

Fig. 15.— Global VLBI image of 1441+52 (3C303) at 5 GHz. The HPBW is 3 × 1 mas in PA 0°. The noise level is 0.05 mJy/beam and levels are: -0.1, 0.1, 0.12, 0.15, 0.2, 0.3, 0.4, 0.6, 0.8, 1, 1.5, 2, 3, 5, 10, 50, and 100 mJy/beam.

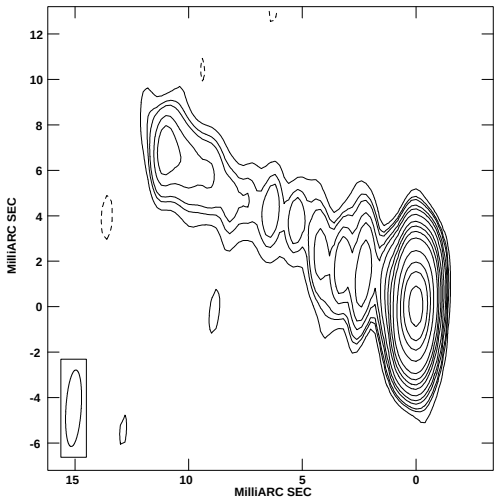

Fig. 16.— Global VLBI image of 1833+32 (3C382) at 5 GHz. The HPBW is 3.4 × 0.7 mas in PA = -4°. The noise level is 0.15 mJy/beam and levels are: -0.5, 0.5, 0.8, 1, 1.5, 2, 3, 5, 7, 10, 15, 30, 50, 70, and 100 mJy/beam.

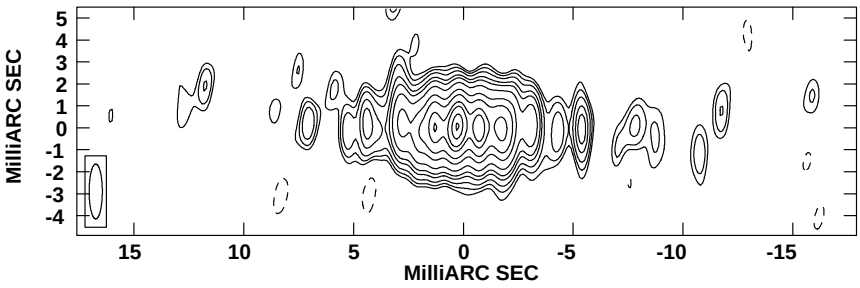

Fig. 17.— Global VLBI image of 2243+39 (3C452) at 5 GHz, uniform weight. The HPBW is 2.5 × 0.6 mas in PA 0°. The noise level is 0.2 mJy/beam and levels are: -0.5, 0.5, 0.7, 1, 1.5, 2, 3, 5, 7, 10, 12, 15, and 17 mJy/beam.

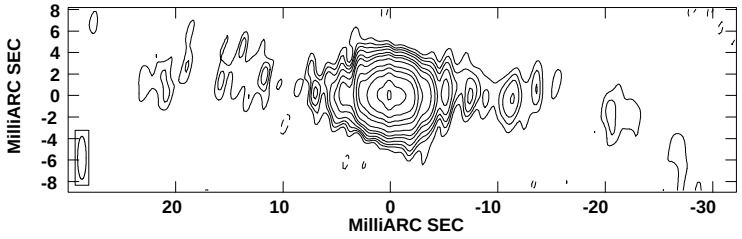

Fig. 18.— Global VLBI image of 2243+39 (3C452) at 5 GHz, natural weight. The HPBW is 4 × 0.8 mas in PA 0°. The noise level is 0.1 mJy/beam and levels are: -0.3, 0.3, 0.5, 0.7, 1, 1.5, 2, 3, 5, 7, 10, 15, and 20 mJy/beam.

REFERENCES

Aaron, S.E.: 1999 A.S.P. Conf. Ser., ed. Leo Takalo, p. 427

Antonucci, R. R. J. 1985 ApJS, 59, 499

Alef, W., Wu, S.Y., Preuss, E., Kellermann, K.I., Qiu, Y.H. 1996 A&A, 308, 376

Barth, A.J., Filippenko, A.V., Moran, E.C. 1999 ApJ, 525, 673

Baum, S.A., O'Dea, C.P., Giovannini, G., Biretta, J., Cotton, W.B., de Koff, S., Feretti, L., Golombek, D., Lara, L., Macchetto, F.D., Miley, G. K., Sparks, W.B., Venturi, T., Komissarov, S.S. 1997 ApJ, 483, 178

Biretta, J.A., Sparks, W.B., Macchetto, F. 1999 ApJ, 520, 621

Chiaberge, M., Celotti, A., Capetti, A., Ghisellini, G., 2000 A&A, 358, 104

Conway, J.E. 1996, 175th IAU Symposium publ. by Kluwer Academic Publ., Ekers, R.D., Fanti, C., and Padrielli, L. eds. p. 92

Cotton, W.D., Feretti, L., Giovannini, G., Venturi, T., Lara, L. 1995, ApJ, 452, 605

Cotton, W.D., Giovannini, G., Feretti, L., Lara, L., Venturi, T. 1999, ApJ, 519, 108

Falcke, H., Nagar, N.M., Wilson, A.S., Ulvestad, J.S. 2000, ApJ, in press. Astro-ph/0005383

Fanaroff, B.L., & Riley, J.M. 1974, MNRAS, 167, 31

Fanti, C., Fanti, R., de Ruiter, H.R., Parma, P. 1986, A&AS, 65, 145

Fanti, C., Fanti, R., de Ruiter, H.R., Parma, P. 1987, A&AS, 69, 57

Fraix-Burnet, D. 1997, MNRAS, 284, 911

Ghisellini, G., Padovani, P., Celotti, A., Maraschi, L. 1993, ApJ, 407, 65

Giovannini, G., Feretti, L., Gregorini, L., Parma, P. 1988 A&A, 199, 73

Giovannini, G., Feretti, L., Comoretto, G. 1990 ApJ, 358, 159

Giovannini, G., Feretti, L., Venturi, T, Lara, L., Marcaide, J., Rioja, M., Spangler, S.R., Wehrle, A.E. 1994, ApJ, 435, 116

Giovannini, G., Cotton, W.D., Feretti, L., Lara, L., Venturi, T, Marcaide, J. 1995, Proc. Natl. Acad. Sci. USA, 92, 11356

Giovannini, G., Cotton, W.D., Feretti, L., Lara, L., Venturi, T. 1998a, ApJ, 493, 632

Giovannini, G., Cotton, W.D., Feretti, L., Lara, L., Venturi, T. 1998b, Proceedings of "32nd COSPAR Scientific Assembly, Nagoya, Japan, Sect. E1.3, Adv. in Space Research, 26, 693

Giovannini, G., Taylor, G.B., Arbizzani, E., Bondi, M., Cotton, W. D., Feretti, L., Lara, L., Venturi, T. 1999a ApJ, 522, 101

Giovannini, G., Feretti, L., Venturi, T., Cotton, W.D., Lara, L. 1999b, A.S.P. Conf. Ser. 159, ed. Leo Takalo, p. 439

Gregory, P. C. & Condon, J. J. 1991 ApJS, 75, 1011

Hardcastle, M. J., Alexander, P., Pooley, G. G., Riley, J. M. 1996, MNRAS, 278, 273

Harris, D.E., Owen, F., Biretta, J.A., Junor, W. 1999 MPE Report 271 Proceedings of the Workshop *Diffuse Thermal and Relativistic Plasma in Galaxy Clusters*, p. 111; H. Boehringer, L. Feretti and P. Schuecker eds.

Homan, D.C., Ojha, R., Wardle, J.F., Roberts, D.H., Aller, M.F., Aller, H.D., Hughes, P.A.: 2000, ApJ, submitted; astro-ph/0009301

Jackson, N., Sparks, W. B., Miley, G. K., Macchetto, F. 1993, A&A, 269, 128

Junor, W., Biretta, J.A., Livio, M. 1999, Nature 401, 891

Laing, R.A. 1996, A.S.P. Conf. Ser. 100, Hardee et al. eds, p. 241

Lara, L., Cotton, W.D., Feretti, L., Giovannini, G., Venturi, T., Marcaide, M. 1997, ApJ, 474, 179

Lara, L., Feretti, L., Giovannini, G., Baum, S., Cotton, W.D., O'Dea, C. P., Venturi, T. 1999 ApJ, 513, 197

Leahy, J.P., Perley, R.A. 1991 AJ, 102, 537

Lobanov, A.P. & Zensus, J.A. 1999, ApJ, 521, 509

Marscher, A.P. 1999, Astrop. Physics, 11, 19

Owen, F., Eilek, J., Kassim, N. 1999 MPE Report 271 Proceedings of the Workshop *Diffuse Thermal and Relativistic Plasma in Galaxy Clusters*, p. 107; H. Boehringer, L. Feretti and P. Schuecker eds.

Pacholczyk, A.G. 1970, Radio Astrophysics, ed. G. Burbidge and M. Burbidge, (San Francisco: Freeman)

Piner, B. G., Unwin, S. C., Wehrle, A. E., Edwards, P. G., Fey, A. L., Kingham, K. A. 1999 ApJ, 525, 176

Rector, T.A., Stocke, J.T., Perlman, E. S. 1999 ApJ, 516, 145

Sanghera, H. S., Saikia, D. J., Luedke, E., Spencer, R. E., Foulsham, P. A., Akujor, C. E., Tzioumis, A. K. 1995 A&A, 295, 629

Schilizzi, R.T., Fanti C., Fanti R., Parma P.: 1983 A&A, 126, 412

Schwab, F.R., & Cotton, W.D., 1983 AJ, 88, 688

Sudou, H., Taniguchi, Y., Ohyama, Y., Kameno, S., Sawada-Satoh, S., Inoue, M., Kaburaki, O., Sasao, T.: 2000, Publ. Astron. Soc. Japan, in press. Astro-ph/0008173.

Tansley, D., Birkinshaw, M., Hardcastle, M.J., Worral, D.M.: 2000, MNRAS, in press. astro-ph/0005272

Urry, C.M., & Padovani, P. 1995, PASP, 107, 803

Venturi, T., Castaldini, C., Cotton, W. D. Feretti, L., Giovannini, G., Lara, L, Marcaide, J. M., Wehrle, A. E. 1995 ApJ, 454, 735

Xu, C., Baum, S.A., O'Dea, C.P., Wrobel, J.M., Condon, J.J.: astro-ph/0009124

AAS LaTeX macros v5.0.